GA–A22206

HIGH HEAT FLUX TESTING OF CFC COMPOSITES FOR THE TPX PHYSICS EXPERIMENT

by
P.G. VALENTINE, R.E. NYGEN, R.W. BURNS, P.D. ROCKET,
A.P. COLLERAINE, R.J. LEDERICH, and JT BRADLEY

FEBRUARY 1996

GA–A22206

HIGH HEAT FLUX TESTING OF CFC COMPOSITES FOR THE TPX PHYSICS EXPERIMENT

by

P.G. VALENTINE, R.E. NYGEN,* R.W. BURNS,† P.D. ROCKET,*
A.P. COLLERAINE, R.J. LEDERICH,† and JT BRADLEY‡

This is a preprint of a paper to be presented at the 7th International Conference on Fusion Reactor Materials, September 25–29, 1995, Obninsk, Russia, and to be published in *The Proceedings.*

*Sandia National Laboratories, Albuquerque, New Mexico.
†McDonnell Douglas Aerospace, St. Louis, Missouri.
‡University of New Mexico, Albuquerque, New Mexico.

Work supported by
the U.S. Department of Energy
under Contract No. DE-AC02-76CH03073

GA PROJECT 3998
FEBRUARY 1996

ABSTRACT

High heat flux (HHF) testing of carbon fiber reinforced carbon composites (CFCs) was conducted under the General Atomics program to develop plasma-facing components (PFCs) for Princeton Plasma Physics Laboratory's Tokamak Physics Experiment (TPX). As part of the process of selecting TPX CFC materials, a series of HHF tests were conducted with the 30 kW Electron Beam Test System (EBTS) Facility at Sandia National Laboratories, and with the Plasma Disruption Simulator I (PLADIS-I) Facility at the University of New Mexico. The purpose of the tests was to make assessments of the thermal performance and erosion behavior of CFC materials. Tests were conducted with 42 different CFC materials. In general, the CFC materials withstood the rapid thermal pulse environments without fracturing, delaminating, or degrading in a non-uniform manner; significant differences in thermal performance, erosion behavior, vapor evolution, etc. were observed and preliminary findings are presented below. The CFCs exposed to the hydrogen plasma pulses in PLADIS-I exhibited greater erosion rates (0.14 to 0.21 gm/MJ) than the CFC materials exposed to the electron-beam pulses in EBTS (0.02 to 0.15 gm/MJ). The results obtained support the continued consideration of a variety of CFC composites for TPX PFC components.

1. INTRODUCTION

The primary goal of the Tokamak Physics Experiment (TPX) is to develop the scientific basis for a compact and continuously-operating tokamak fusion reactor [1]. Because the TPX tokamak will have long pulse capability (≥1000 s) and must accommodate high heat loads (up to 7.5 MWm^{-2}), active cooling of the PFCs is required.

Two of the major issues associated with the selection of the CFC materials are the erosion behavior of the CFCs and their ability to be joined to copper tubing and plates [2]. Plasma-facing materials for TPX must have the following characteristics: (1) high thermal conductivity, particularly in the direction perpendicular to the PFC faces; (2) mechanical integrity at high temperatures; and (3) compositions consisting of only low atomic number elements. CFCs were chosen as the best type of material to meet these requirements. The total plasma-facing surface area of the PFCs will be approximately 110 m^2 and will require the use of roughly 5800 kg of CFC materials. Because the D-D (deuterium-deuterium) environment of TPX will achieve a fluence of only about 1×10^{-4} dpa (displacements per atom), neutron damage of the CFCs is estimated to reduce the CFC thermal conductivity by less than 10%. The TPX tokamak will be the first machine designed to allow a substantial amount of CFC erosion (up to 7 mm) over the lifetime of the reactor.

As part of the process of selecting TPX CFC materials, high heat flux (HHF) tests were conducted with the Electron Beam Test System (EBTS) Facility at Sandia National Laboratories, and with the Plasma Disruption Simulation I (PLADIS-I) Facility at the University of New Mexico. A total of 57 uncooled specimens were tested in the EBTS facility; nine additional specimens were tested in the PLADIS-I facility.

2. MATERIALS AND EXPERIMENTAL PROCEDURES

2.1. Materials and test specimen preparation

For these HHF tests, 42 different CFC materials were provided by 19 CFC manufacturers (Table 1). From these materials, 25 mm x 25 mm x 10 mm test specimens were machined using a carbide flycutter on a milling machine. In order to assess how CFC anisotropy influences performance, multiple types (orientations) of test specimens were fabricated from some of the materials such that the performance of the CFCs could be examined in more than one direction. After machining, the specimens were ultrasonically cleaned in ethyl alcohol and then heat treated at 1100˚C in vacuum for at least three hours to remove volatiles and high vapor pressure impurities.

2.2. Microstructural characterization methods

Scanning electron microscopes (SEMs), with energy dispersive X-ray analysis (EDX) capabilities, and reflected-light microscopes were employed to examine both the surfaces and cross sections of the test specimens before and after exposure in the EBTS and PLADIS-I facilities.

2.3. EBTS tests

Two series of electron-beam tests were conducted using the 30 kW EBTS [3]. In the first series of e-beam tests 26 CFC specimens were exposed to power densities up to 92 MW/m^2 (Table 2); in the second series of tests, 31 CFC specimens were exposed to power

Table 1

Summary of the 49 CFC Materials Tested in the EBTS and PLADIS-I Facilities. The test specimen thermal conductivities (k_z) in the direction parallel to the e-beam or plasma-beam are listed at right. F = fiber reinforcement type [proprietary, rayon, PAN, pitch, or vapor-grown carbon fiber (VGCF)]. M = matrix type [none, proprietary, resin, CVI, or pitch].

Manufacturer	Description	Architecture	k_z (at 20˚C)
Aerotherm Corporation	HiCond; F = Pitch, M = Pitch	2D	300
	SSN; F = PAN, M = Pitch	3D	220
Alliant Techsystems Inc. (Hercules Aerospace Co.)	ATI 1D; F = Pitch, M = Unknown	1D	Unknown
	HA-PAN 334; F = PAN, M = Pitch	3D	103
	(a) HA-K334; F = Pitch, M = Pitch	3D	170 or 270
	(b) HA-K334; F = Pitch, M = Pitch	3D	270
AlliedSignal Inc.	865-19-4; F = Pitch, M = CVI	3D	221
Amoco Performance Products, Inc.	(a) ThermalGraph 8000 Panel; F = Pitch, M = None	1D	25
	(b) ThermalGraph 8000 Panel; F = Pitch, M = None	1D	750
Applied Sciences, Inc.	ASI 1D; F = VGCF, M = CVI+Pitch	1D	900
BF Goodrich Aerospace	BFG 1D; F = Pitch, M = CVI+Pitch	1D	650
	(a) C-251 Hi-K Unbalanced Weave; F = PAN, M = CVI	2D	89
	(b) C-251 Hi-K Unbalanced Weave; F = PAN, M = CVI	2D	235
	(a) AL-C; F = PAN, M = CVI	3D	215
	(b) AL-C; F = PAN, M = CVI	3D	235
	(a) Super-Carb; F = PAN, M = CVI	3D	156
	(b) Super-Carb; F = PAN, M = CVI	3D	219
BP Chemicals (Hitco) Inc.	Type CC363A; F = Pitch, M = CVI	3D	110
Carbon-Carbon Advanced Technologies, Inc.	F-23; F = Pitch, M = Resin	2D	Unknown
Carbone of America	AEROLOR A05; F = PAN, M = CVI	2D	100
Dunlop Limited / Aviation Division	ATG; F = PAN, M = CVI	2D	330
	DMS 704; F = PAN, M = CVI	2D	210
	ATA; F = PAN+Pitch, M = CVI	3D	351
Fiber Materials, Inc.	(a) 2-2-2 Fine Weave, Type A; F = Pitch, M = Pitch	3D	Unknown
	(b) 2-2-2 Fine Weave, Type A; F = Pitch, M = Pitch	3D	Unknown
	(c) 2-2-2 Fine Weave, Type A; F = Pitch, M = Pitch	3D	120
	2-2-3 Fine Weave; F = PAN, M = Pitch	3D	120
	2-2-2 Fine Weave, Type B; F = Pitch, M = Pitch	3D	220
	3D P-120; F = Pitch, M = Pitch	3D	280
	3D High Conductivity; F = Pitch, M = Pitch	3D	450
	4D Coarse Weave; F = Pitch, M = Pitch	4D	145
	4D Fine Weave; F = Pitch, M = Pitch	4D	145
Kaiser Aerotech	K-Karb 188; F = Pitch, M = Pitch	1D	550
	Type A K-Karb; F = Rayon, M = Resin+Pitch	2D	14
	K-Karb 102HS; F = PAN, M = Resin+Pitch	3D	40
Mitsubishi Chemical America, Inc.	MFC-1; F = Pitch, M = Proprietary	1D	550
	MFC-3(2); F = Pitch, M = Proprietary	3D	210
Science Applications International Corporation	SAIC 1D Rod; F = PAN, M = CVI+Pitch	1D	120
	ISOCARB 140/PAN; F = PAN, M = Resin+Pitch	4D	91
	ISOCARB 140/Pitch; F = Pitch, M = Resin+Pitch	4D	111
Sigri Great Lakes Carbon Corporation	SIGRABOND 1002 ZV 22; F = PAN, M = Resin+Pitch	2D	40
	SIGRABOND 1502 ZV 22; F = PAN, M = Resin+Pitch	2D	30
Société Européenne de Propulsion	SEPCARB N11-011; F = PAN, M = CVI	3D	220
	SEPCARB N21; F = PAN, M = CVI	3D	240
Textron Specialty Materials	Multidimensional Tile; F = Pitch, M = CVI	3D	102
	High HT Temp. Multidimensional Tile; F = Pitch, M = CVI	3D	>102
Tonen Corporation	FC-1030X; F = Pitch, M = Resin+Pitch	1D	493
Toyo Tanso USA, Inc.	CX-2002U; F = Pitch, M = CVI	2D	400
	CX-3002U; F = Pitch, M = CVI	2D	410

Table 2

EBTS Test Matrix For 1st Series of Electron-Beam Experiments

Case No.	Heat Flux (MW/m^2)		Duration (s)
	Nominal	Actual	
1	2.5	2.5	1.5
2	5.0	5.0	1.5
3	7.5	7.5	1.5
4	15.0	15.0	1.5
5	30.0	30.0	1.5
6	45.0	45.0	1.5
7	60.0	60.0	1.5
8	75.0	75.0	1.5
9	90.0	65.0	1.5
10	105.0	92.0	1.5

Note: For each case, each specimen received one e-beam pulse. Once a specimen reached 2600˚C during a specific case, it was dropped from testing in subsequent cases.

densities up to 110 MW/m^2. Test specimens were placed in a graphite specimen holder on a water-cooled, computer-controlled, x-y table. A background pressure of 6×10^{-4} Pa was maintained in the test chamber using a cold-trapped diffusion pump. Tests were observed using both visible-light and infrared (IR) cameras. In conjunction with the IR camera, optical and IR pyrometers were used to monitor specimen surface temperatures over a range of 20˚ to 3000˚C. Instead of monitoring only the overall chamber pressure, a residual gas analyzer (RGA) was used in the second series of tests to assess the volume and composition of the vapors being released from the specimens. For both series of tests the e-beam spot size was 8 mm; the beam was rastered over a 100 mm^2 area (nominally a 10 mm x 10 mm square). Testing was performed such that if a specimen surface temperature exceeded 2600˚C, the e-beam was automatically turned off. For the first series of tests, once a specimen exceeded the preset 2600˚C temperature limit, it was no longer tested in subsequent, higher heat flux, test cases. This affected eight of the 26 specimens in the first series of tests. In the second series, all specimens were subjected to each of the different test cases.

2.4. PLADIS-I tests

One series of plasma disruption simulation tests were conducted using the PLADIS-I facility [4]. For these tests, which used hydrogen discharges, the nine CFC specimens were placed 105 mm from the gun and exposed one at a time. Specimens were held on two sides and sat on a ceramic pedestal. Each of the specimens tested received ten 100-μs pulses; two of the specimens each received an additional ten 100-μs pulses (for a total of 20 pulses). The spot size was approximately 23 mm in diameter and the energy density was 11.5 MJ/m^2; the deposited energy was 4.8 kJ per pulse. This was verified by performing similar plasma pulses with a calorimeter and through the use of copper witness plates. As with the EBTS tests, specimen weight losses were measured using a calibrated laboratory balance.

3. RESULTS AND DISCUSSION

3.1. EBTS tests

The results of the first of the two series of e-beam tests (see Sec. 2) are presented below (a more comprehensive report, including the second series of e-beam tests, will be published later).

Each of the specimens was subjected to up to ten 1.5-second e-beam pulses, which ranged in power density from 2.5 to 92.0 MW/m^{-2} (Table 2). For a specimen which was subjected to all ten full-length pulses, the total deposited energy was approximately 60 kJ. A fraction of this energy (estimated to be 10%–15 % for a typical specimen) goes into heating the bulk material while the remainder raises the surface temperature to the point where erosion (by carbon vaporization) becomes significant. All 26 specimens performed well. No thermal shock damage was observed in any of the specimens. No catastrophic failures occurred and no evidence of e-beam induced cracking was found in any of these unconstrained test specimens. Differences in erosion rates and mechanisms were evident, as were differences in the thermal conductivity/capability of the various materials tested.

From the weight loss data, it is evident that under similar conditions there can be substantial differences in the erosion rates of different CFC materials and that for the same CFC material, tested in multiple orientations, significant differences in performance can occur. Eighteen of the 26 specimens were exposed to all ten of the e-beam pulses shown in Table 2. Because of their low thermal conductivities, the other eight specimens were not subjected to the highest heat fluxes in order to prevent coating of diagnostic ports with

carbon from excessive specimen vaporization. For those specimens exposed to the entire series of 10 e-beam pulses, the total weight losses varied from 0.90 mg to 5.48 mg. The smallest weight loss occurred with the Dunlop ATA CFC. The results of the best performing CFCs, in terms of their ability to remove heat from the 100 mm^2 e-beam exposed region, are summarized in Fig. 1. Considering only those pulses which raised the CFC surface temperature above 1500˚C, the erosion rates were calculated to be in the range of 0.02 to 0.15 gm/MJ of energy absorbed (a minimum of 1500˚C was chosen because the carbon vapor pressure is only 1.6 x 10^{-8} Pa at this temperature).

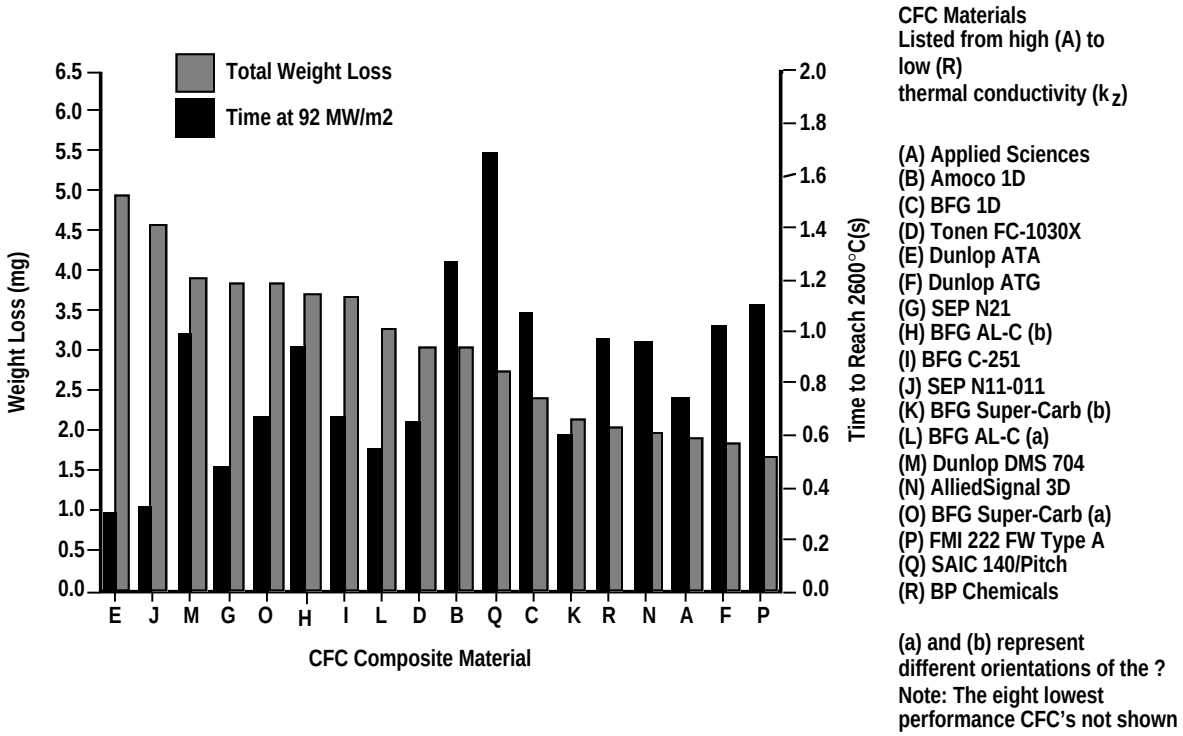

Fig. 1. EBTS e-beam test results. The total weight loss for each of the 18 CFC specimens exposed to the entire series of 10 e-beam pulses is shown. In general, the weight loss increases from left to right for the 18 CFCs, which are listed at the right in terms of high to low thermal conductivity. As a measure of the overall thermal performance of the CFCs, the time required for the specimen surfaces to reach 2600˚C when exposed to a heat flux of 92 MW/m^2 is also shown. The nominal size of the e-beam heated area was 1 cm x 1 cm. The material with the best thermal performance, the Dunlop ATA 3D CFC, is shown at left. The time required to reach 2600˚C decreases from left to right as the overall thermal performance decreases.

In the context of the present study, the thermal performance of a CFC refers to its ability to remove heat from the approximately 10 mm x 10 mm square surface region which was exposed to the EBTS e-beam. Because the overall test specimen face is 25 mm x 25 mm, the thermal performance therefore is a measure of the CFC's ability to conduct heat in all directions simultaneously. This appears to be the primary reason why some of the CFCs with very high thermal conductivity in the through-the-thickness direction (z-direction) did not perform as well as some of the CFCs with lower z-direction conductivity (k_z). For example, the Applied Sciences 1-D CFC, which had the highest k_z of all the CFCs tested (900 W/m-K), had a lower thermal performance than many of the other CFCs tested in EBTS (see Fig. 1); the Dunlop ATA 3-D CFC, which had a k_z of 351 W/m-K, had the highest thermal performance of all the CFCs tested.

For some of the CFC's e-beam tested in multiple orientations, the level of erosion was found to be highly dependent on how the composite fiber architecture was aligned with respect to the e-beam. This was observed previously in a study by Bolt et al. [5] in which the exposed specimen surfaces were smaller than the e-beam cross-sectional area. In contrast to Bolt's findings, some of the 2-D-based CFCs (such as the BF Goodrich Aerospace needled 3-D AL-C CFC) exhibited substantially greater erosion rates when the constituent 2-D plies were aligned parallel to the electron-beam (see material "H" in Fig. 1). For this same BF Goodrich material, when the 2-D plies were aligned perpendicular to the e-beam (see material "L" in Fig. 1) the erosion rate was considerably less (42% less). This significant difference in erosion behavior for the two orientations of this CFC is thought to be due primarily to the low tensile strengths of this CFC in combination with the EBTS test set-up which allows heat flow in directions perpendicular to the e-beam. For the strong Fiber Materials, Inc. (FMI) 2-2-2 Fine Weave CFC tested in three different orientations [with the e-beam aligned with the material's high conductivity direction (z-direction) and with the e-beam oriented at 22.5˚ and also at 45.0˚ from the z-direction], it was observed that in the

higher thermal conductivity orientation, the thermal performance was greater and the erosion rate was less. These results indicate the importance both of in-plane thermal conductivity (perpendicular to the e-beam) for removing heat from high temperature regions, and of CFC mechanical properties for maintaining the structural integrity of the materials.

Using SEM and EDX techniques, analysis of the post-test specimen surfaces and of cross-sections of the specimens was performed. The different constituent materials in the individual composites (i.e., fiber and matrix material) often eroded at different rates [6,7]. In general, for those CFC's made using either PAN- (polyacrylonitrile) or pitch-based fibers in a chemical vapor infiltration (CVI) matrix, the fiber material eroded faster than the matrix material, leaving hollow matrix "shells" in which the fibers had receded. For those CFCs made using pitch-based fibers in a resin- or resin-plus-pitch-based matrix, the matrix eroded faster than the reinforcing fibers. Thus, as might be expected, the constituent material having the higher thermal conductivity, in general, was more erosion resistant. Note that, generally, high conductivity pitch fibers were used in resin/pitch matrices while lower conductivity pitch fibers were used in CVI matrices. Typically, in-plane fiber bundles were observed to erode faster than through-the-thickness fiber bundles.

The EDX examinations found trace levels of impurities in approximately half of the test specimens prior to e-beam testing. After testing, the impurities were gone in the specimen regions which had been affected by the e-beam pulses. Typically, the impurities were one or more of the following: calcium, copper, sulfur, and silicon.

3.2. PLADIS-I tests

The plasma-beam tests were performed using nine CFC specimens (see Fig. 2). Most of the CFC materials tested had essentially identical weight losses per pulse (nominally

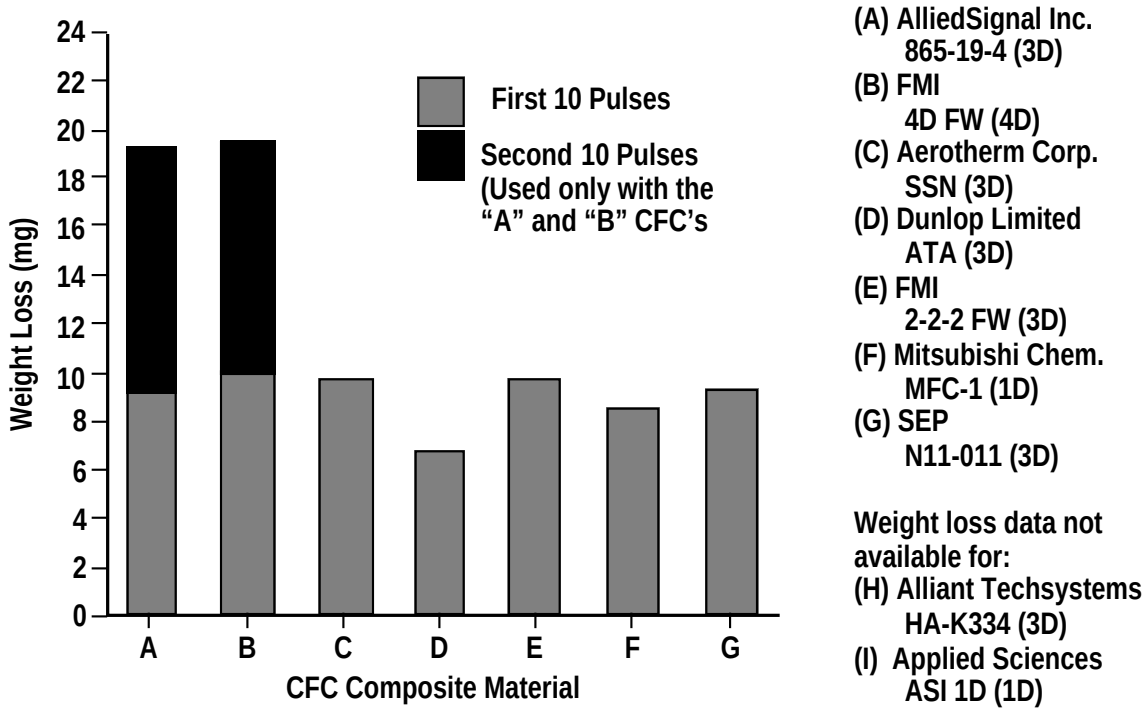

Fig. 2. PLADIS-I hydrogen plasma disruption simulation test results. The total weight loss for seven of the nine CFC specimens exposed to a series of 100-μs hydrogen plasma pulses is shown. Specimen weight loss is relatively insensitive to CFC type or thermal conductivity in the direction parallel to the plasma beam. However, there are two exceptions: the two highest conductivity materials (Dunlop ATA 3-D and Mitsubishi MFC-1 1-D) eroded at rates less than those observed with the other five CFCs shown (32% and 13%, respectively). Each plasma pulse had an energy density of 11.5 MJ/m^2; the plasma beam had a nominal diameter of 23 mm.

0.95 mg) and eroded at a rate of 0.21 gm/MJ of absorbed energy. This erosion rate is consistent with earlier work performed with the PLADIS-I facility in which three different CFCs were found to have erosion rates ranging from 0.08 to 0.37 gm/MJ for single pulse exposures [8]. The 0.21 gm/MJ rate is approximately twice the rate observed for the 1.5 s pulse, e-beam test specimens. This appears reasonable in light of the significant shock loading which the specimens received from the 100-μs PLADIS-I pulses. Furthermore, both because of the hydrogen ions' greater mass and lesser penetrating ability (vs. that of the EBTS electrons) and the minimal amount of time available for heat conduction, significant vaporization and erosion of the CFC surface layers were expected and observed in the PLADIS-I tests.

Two of the CFCs tested in PLADIS-I had significantly less weight loss than the other CFCs tested. These two materials, the Dunlop ATA and the Mitsubishi MFC-1, lost 0.65 mg per pulse and 0.83 mg per pulse, respectively. The only obvious difference between the two more erosion resistant CFCs and the others is that the two better performing materials (in terms of erosion) had higher thermal conductivities in the direction parallel to the plasma beam. The Dunlop ATA had a k_z = 351 W/m-K and the Mitsubishi MFC-1 had a k_z = 550 W/m-K. The others, not counting the two for which weight loss data are not available, had k_zs between 145 and 221 W/m-K. A prior investigation [9] also reported that as the thermal conductivity of graphites and CFCs increases, their resistance to erosion by hydrogen plasma pulses increases.

The FMI 4-D Fine Weave CFC and the AlliedSignal Inc. 865-19-4 CFC specimens each received 20 pulses in groups of 10 pulses at a time; both groups of 10 pulses had essentially the same effect on the two specimens.

One of the two 1-D CFCs tested in PLADIS-I did not withstand the impulse loading as well as the other CFCs tested. The Applied Sciences 1-D CFC fractured into three pieces during testing and additional cracking occurred within the three pieces.

Using SEM and EDX techniques, analysis of the post-test specimen surfaces and of cross-sections of the specimens was performed. Ignoring the slight amount of contamination present from the PLADIS-I gun, the primary observation is that all of the materials eroded in a similar, very uniform manner (see Fig. 3).

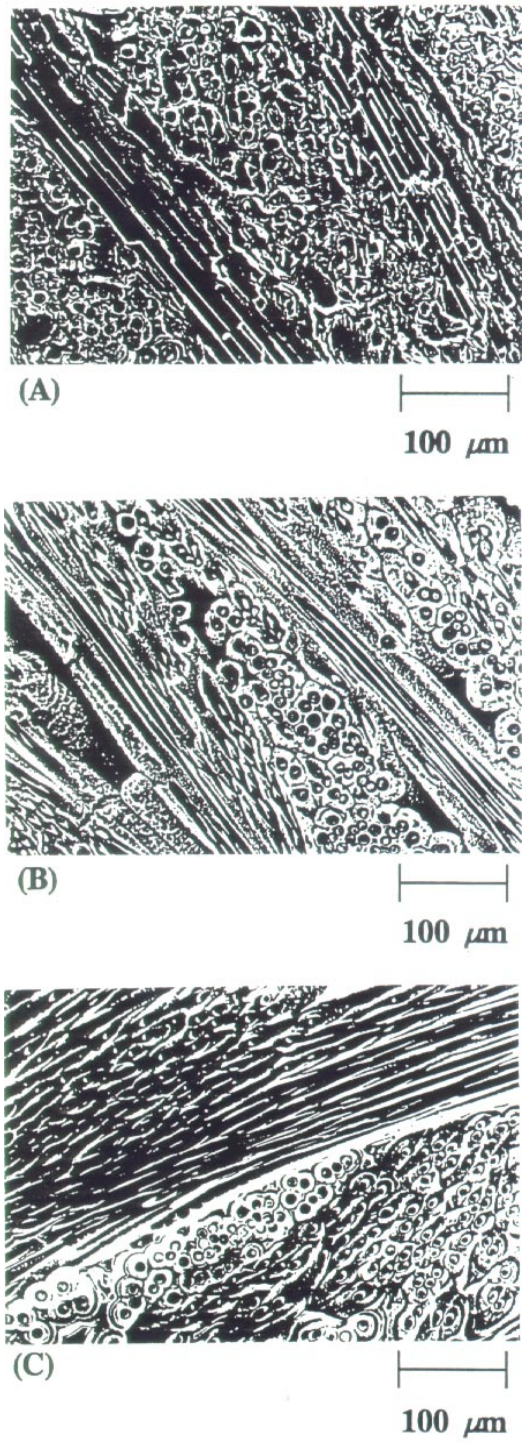

Fig. 3. Surface microstructures of three different AlliedSignal Inc. 865-19-4 3D CFC test specimens. The three secondary-electron SEM images provide a comparison of the specimen surfaces after they have received the following: (a) machining to test specimen geometry; (b) exposure to the ten e-beam pulses listed in Table 2; and (c) exposure to twenty 100-μs hydrogen-plasma pulses at an energy density of 11.5 MJ/m^2. Note the following: the fractured fibers and matrix material, typical of a machined surface, in (a); the preferential erosion of fibers, compared to matrix, in (b); and the very smooth, uniformly-eroded fibers and matrix in (c).

4. SUMMARY AND CONCLUSIONS

Results of the high heat flux experiments conducted using the EBTS and PLADIS-I test facilities showed that, while almost all of the 42 CFC materials tested have excellent resistance to failure by thermal shock, the thermal performance and erosion behavior of the materials can vary significantly. None of the CFCs showed evidence of e-beam induced cracking or catastrophic failure. Only one of the materials (a 1-D CFC) exhibited evidence of cracking in the PLADIS-I plasma disruption simulation tests (the CFC fractured into several pieces).

From the EBTS e-beam tests, the importance of both through-the-thickness and in-plane thermal conductivity on the overall thermal performance of the CFCs could be seen by the varying rates at which the difference materials heated up and by the maximum temperatures which were reached for a specific heat flux. The e-beam test results also indicate that when a CFC has significant differences in fiber architecture in the x-, y-, and z-directions, (for example: a needled 3-D CFC, which has only minor reinforcement in the third direction, as compared to a fully woven balanced 3-D CFC), the erosion rate can depend greatly on orientation. For TPX PFC components, the CFC materials are predicted to experience substantial erosion (up to 7 mm). Therefore, orientation-dependent properties and erosion rates should be considered as important parameters in the selection of PFC CFC materials and in the development of composite material performance predictions.

The materials which performed the best in the EBTS tests, in terms of both thermal performance (lowest surface temperature) and erosion resistance, were the Dunlop Limited ATA 3D CFC and the Société Européenne de Propulsion N11-011 3D CFC. The best

performing material in the PLADIS-I tests, in terms of erosion resistance, was the Dunlop Limited ATA 3D CFC.

The results of the electron-beam and plasma disruption simulation tests indicate a variety of CFC composite types, of varied fiber architecture and fiber/matrix constituent material combinations, are suitable for consideration in TPX PFC designs. Additional efforts are required to more fully assess the best candidate CFC types and to evaluate the performance of brazed CFC's for use as HHF plasma-facing armor and divertor components.

REFERENCES

[1] W.T. Reiersen and The TPX Team, 15th IEEE/NPSS Symp. on Fusion Engineering, (Institute of Electrical and Electronics Engineers, Inc., Piscataway, New Jersey) Vol. 1, p. 387 (1994).

[2] P.W. Trester, P.G. Valentine, E. Chin, E.E. Reis, and A.P. Colleraine, “Tensile Fracture Characterization of Braze Joined Copper-to-CFC Coupon Assemblies,” this conference.

[3] D.L. Youchison, J.M. McDonald, L.S. Wold; "High Heat Flux Testing Capabilities at Sandia National Laboratories — New Mexico;" ASME Heat Transfer in High Heat Flux Systems; HTD-Vol. 301 (1994) p. 31.

[4] D.Y. Cheng, Nucl. Fusion **10** (1970) 305.

[5] H. Bolt, A. Miyahara, T. Kuroda, O. Kaneko, Y. Kubota, Y. Oka, K. Sakurai; "High Heat Flux Experiments on C-C Composite Materials by Hydrogen Beam at the 10 MW Neutral Beam Injection Test Stand of the IPP Nagoya;" *** need actual journal paper, I have only a pre-journal draft ***; approx. May 1987.

[6] M. Akiba, M. Araki, S. Suzuki, H. Ise, K. Nakamura, K. Yokoyama, M. Dairaku, S. Tanaka; "Experimental and Analytical Studies on Thermal Erosion of Carbon-Based Materials with High Thermal Conductivity;" J. Nucl. Mater. **191–194** (1992) 373.

[7] C.D. Croessmann, N.B. Gilbertson, R.D. Watson, J.B. Whitley; "Thermal Shock Testing of Candidate Compact Ignition Tokamak Graphites;" Fusion Technol. **15** (1989) 127.

[8] S. Suzuki, J.F. Crawford, J.T. Bradley III, J.M. Gahl, and R. Nygren; "Experimental Study of Pulse Plasma Heat Flux Absorption and Ablation During the Simulation of a Tokamak Plasma Disruption;" J. Nucl. Mater. **200** (1993) 265.

[9] J. Linke, V.R. Barabash, H. Bolt, A. Gervash, I. Mazul, I. Ovchinnikov, and M. Rödig; "Erosion of Metals and Carbon Based Materials During Disruptions — Simulation Experiments in Plasma Accelerators;" J. Nucl. Mater. **212–215** (1994) 1195.

ACKNOWLEDGMENTS

The authors gratefully acknowledge the efforts of the following personnel. At General Atomics: N.D. Blatchford, R.R. Enriquez, R.O. Harrington, Jr., W.E. Simpson, R.F. Stetson, P.W. Trester, and D.R. Wall. At Sandia National Laboratories: F. Bauer, K. Trancosa, L. Wold. At the University of New Mexico: J.M. Gahl. The contribution of the CFC materials by the composite material manufacturers is greatly appreciated. This work was supported by the U.S. Department of Energy under Contract No. DE-AC02-76CH03073, Princeton Plasma Physics Laboratory TPX Subcontract S-03756-K.